Supplementary Material (ESI) for Lab on a Chip

The Change of Activation Energy in Microchannel Laminar Flow as Demonstrated by Kinetic Analysis of DNA duplex-coil Equilibrium

Kenichi Yamashita, [a] Masaya Miyazaki, [a,b] Yoshiko Yamaguchi, [a] Hiroyuki Nakamura, [a] and Hideaki Maeda* [a,b,c]

[a] Micro- & Nano-space Chemistry Group, Nanotechnology Research Institute, National Institute of Advanced Industrial Science and Technology (AIST), 807-1, Shuku-machi, Tosu, Saga 841-0052, Japan. Fax: (+81)942-81-3657; Tel: (+81)942-81-3676; E-mail: h.maeda@m.aist.go.jp
[b] Graduate School of Engineering Sciences, Kyushu University, 6-1, Kasuga-Kouen, Kasuga, Fukuoka 816-8580, Japan.
[c] CREST, JST

Article Ref: B800986D

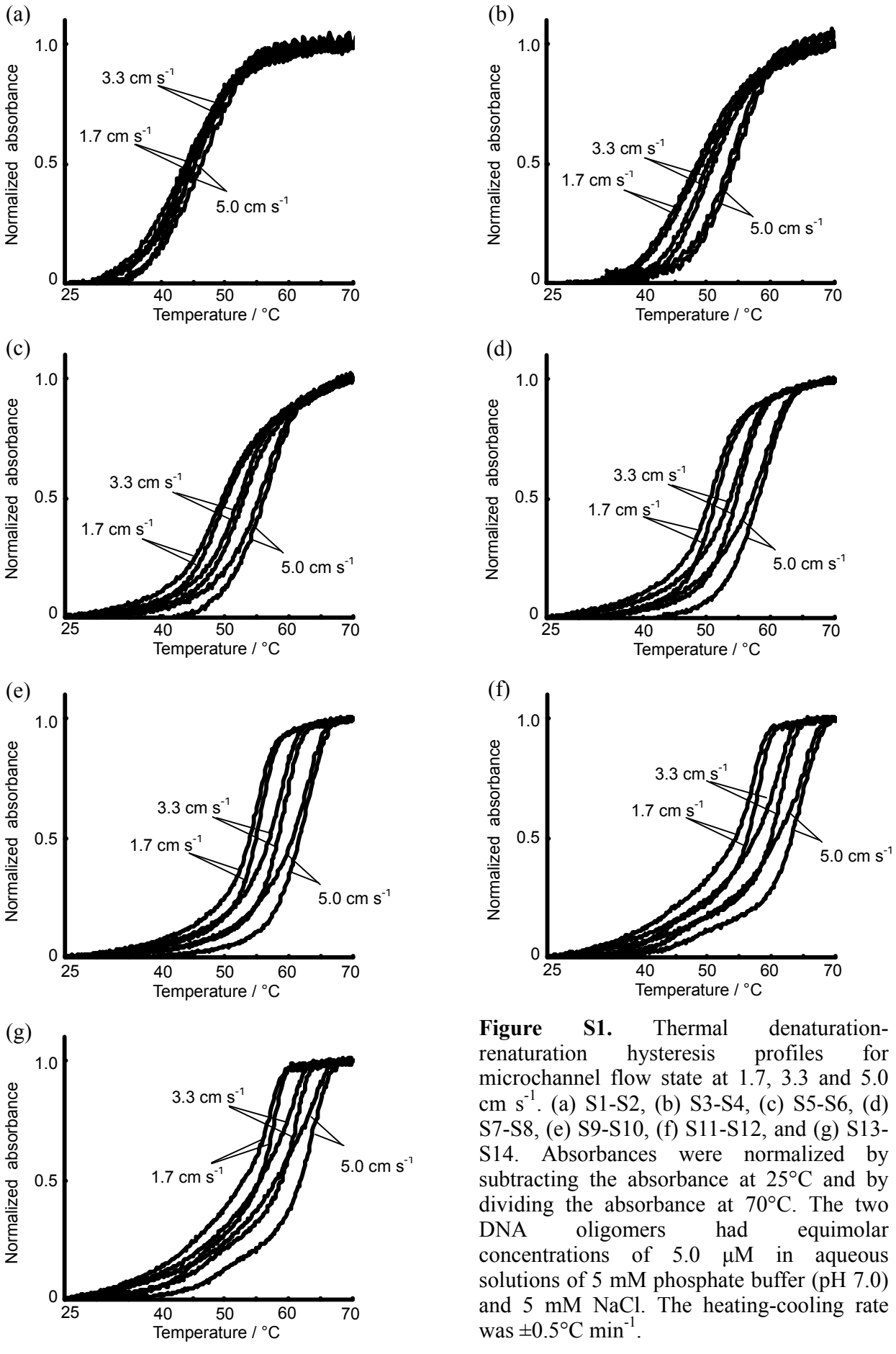

Figure S1. Thermal denaturation-renaturation hysteresis profiles for microchannel flow state at 1.7, 3.3 and 5.0 cm s^{-1}. (a) S1-S2, (b) S3-S4, (c) S5-S6, (d) S7-S8, (e) S9-S10, (f) S11-S12, and (g) S13-S14. Absorbances were normalized by subtracting the absorbance at 25°C and by dividing the absorbance at 70°C. The two DNA oligomers had equimolar concentrations of 5.0 μM in aqueous solutions of 5 mM phosphate buffer (pH 7.0) and 5 mM NaCl. The heating-cooling rate was ±0.5°C min^{-1}.

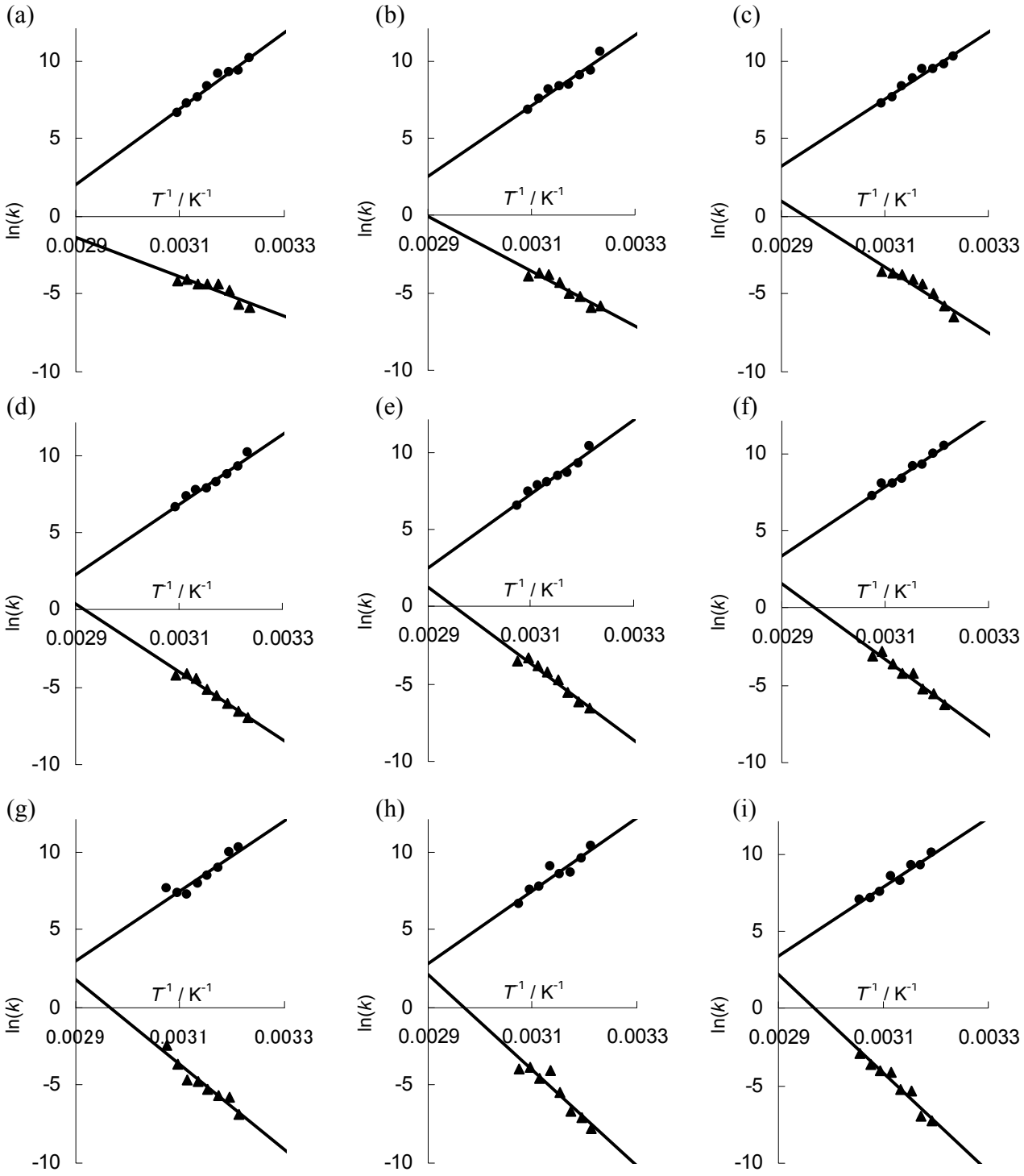

Figure S2-1. Arrhenius plots of S1-S2 of (●) association and (▲) dissociation for (a) batchwise or microchannel flow state at (b) 0.7 cm s^{-1}, (c) 1.7 cm s^{-1}, (d) 2.3 cm s^{-1}, (e) 3.3 cm s^{-1}, (f) 4.2 cm s^{-1}, (g) 5.0 cm s^{-1}, (h) 5.8 cm s^{-1}, and (i) 6.7 cm s^{-1}. The lines are least-squares fits of the data.

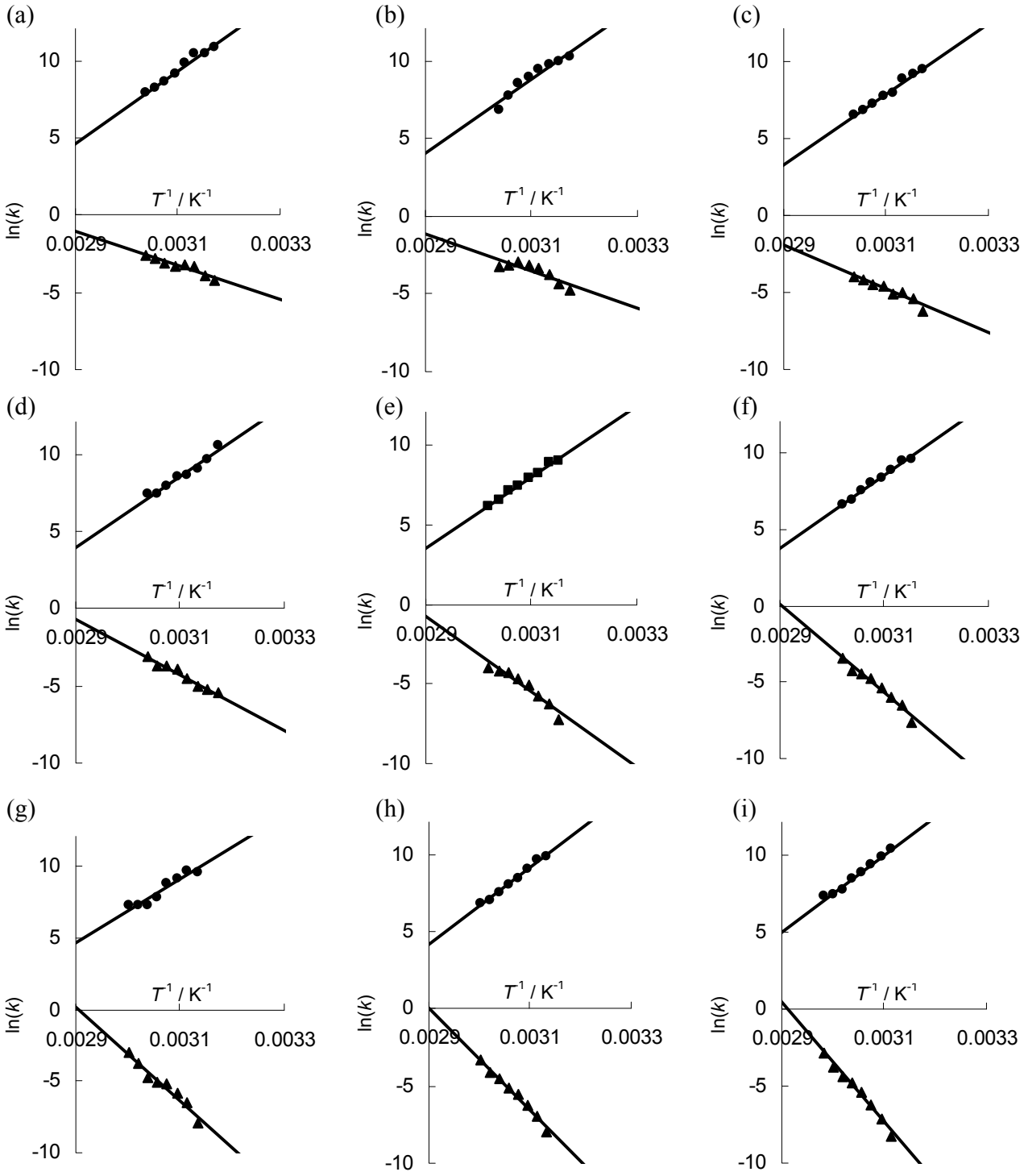

Figure S2-2. Arrhenius plots of S3-S4 of (●) association and (▲) dissociation for (a) batchwise or microchannel flow state at (b) 0.7 cm s^{-1}, (c) 1.7 cm s^{-1}, (d) 2.3 cm s^{-1}, (e) 3.3 cm s^{-1}, (f) 4.2 cm s^{-1}, (g) 5.0 cm s^{-1}, (h) 5.8 cm s^{-1}, and (i) 6.7 cm s^{-1}. The lines are least-squares fits of the data.

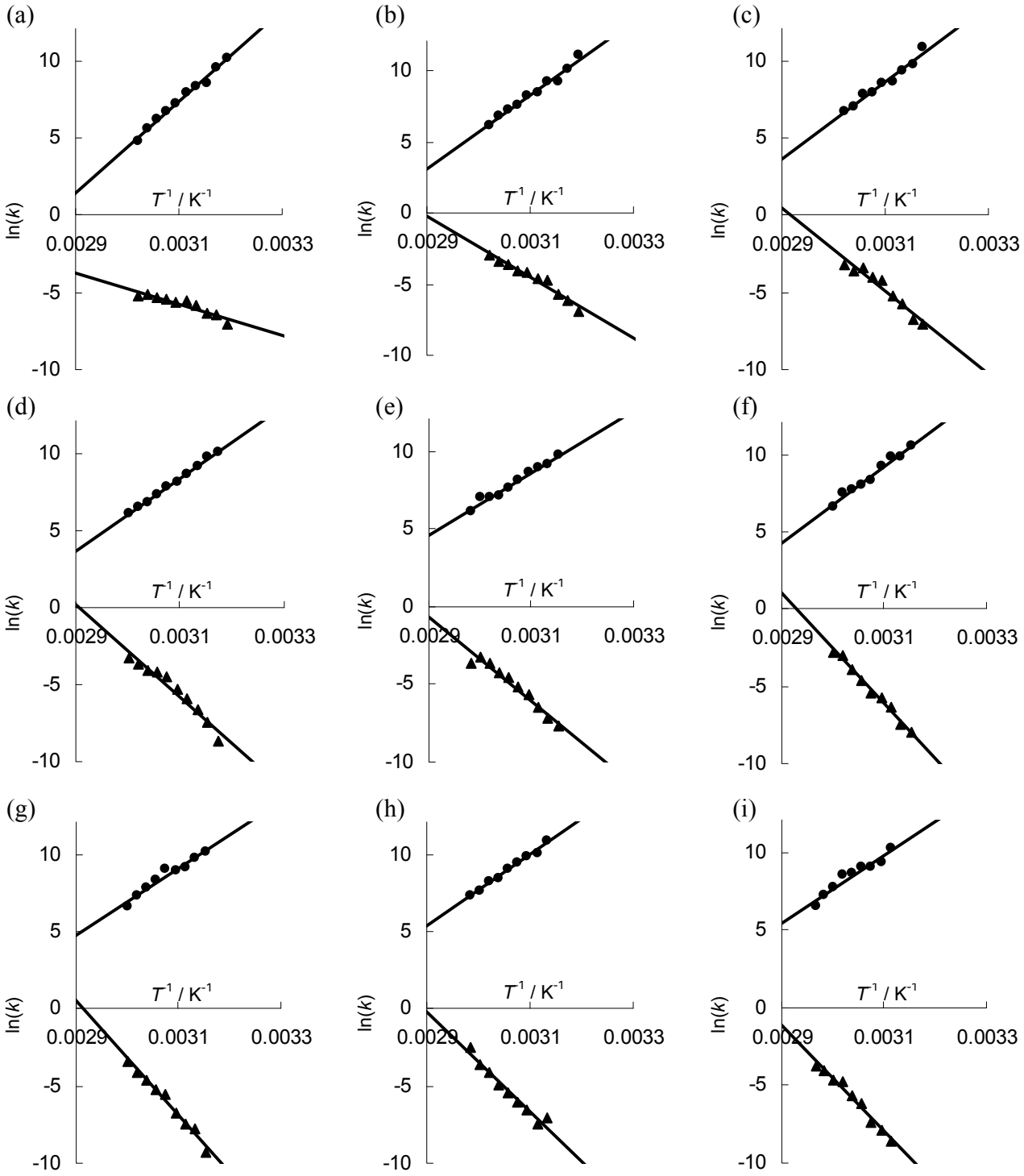

Figure S2-3. Arrhenius plots of S5-S6 of (●) association and (▲) dissociation for (a) batchwise or microchannel flow state at (b) 0.7 cm s^{-1}, (c) 1.7 cm s^{-1}, (d) 2.3 cm s^{-1}, (e) 3.3 cm s^{-1}, (f) 4.2 cm s^{-1}, (g) 5.0 cm s^{-1}, (h) 5.8 cm s^{-1}, and (i) 6.7 cm s^{-1}. The lines are least-squares fits of the data.

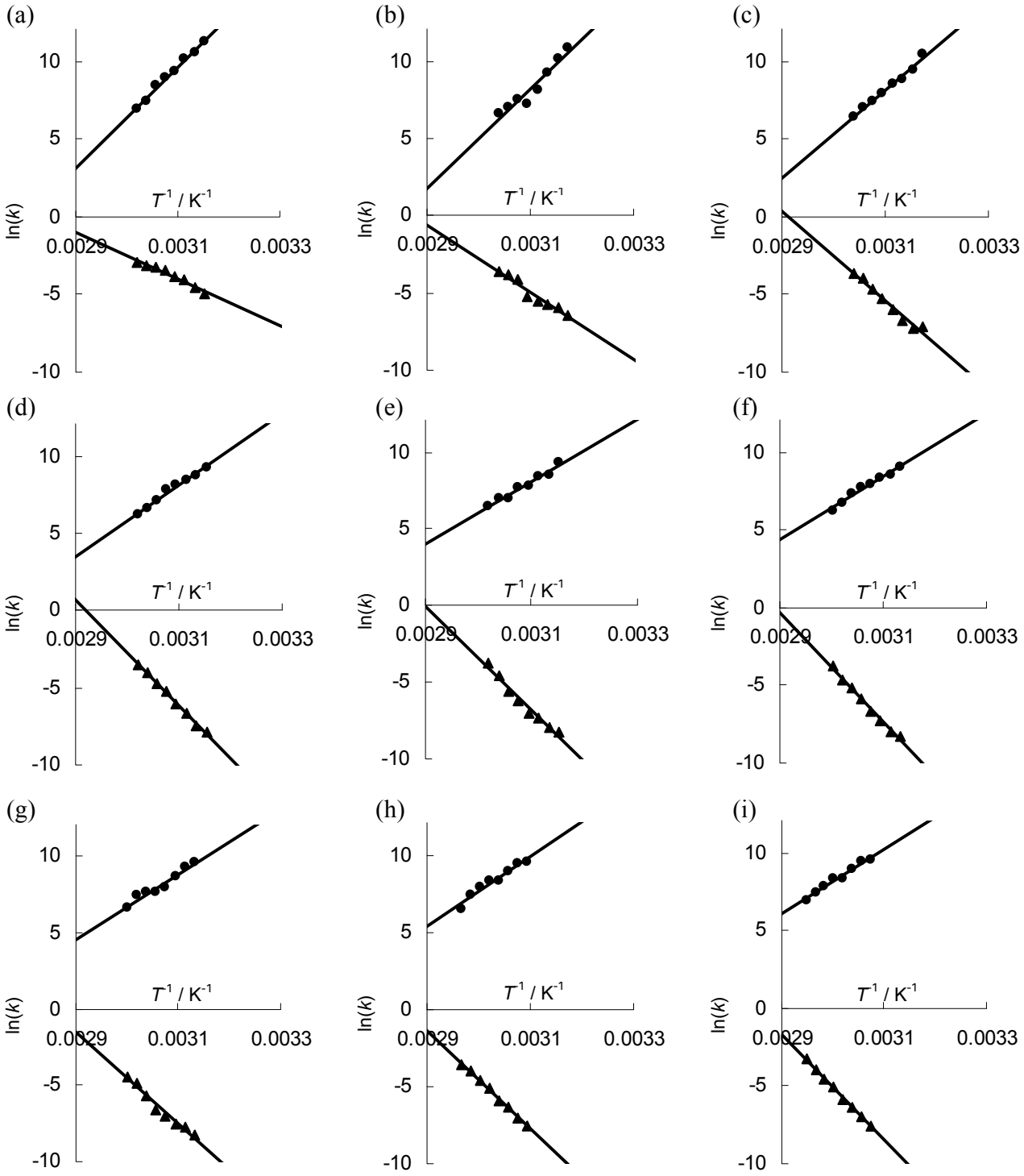

Figure S2-4. Arrhenius plots of S7-S8 of (●) association and (▲) dissociation for (a) batchwise or microchannel flow state at (b) 0.7 cm s^{-1}, (c) 1.7 cm s^{-1}, (d) 2.3 cm s^{-1}, (e) 3.3 cm s^{-1}, (f) 4.2 cm s^{-1}, (g) 5.0 cm s^{-1}, (h) 5.8 cm s^{-1}, and (i) 6.7 cm s^{-1}. The lines are least-squares fits of the data.

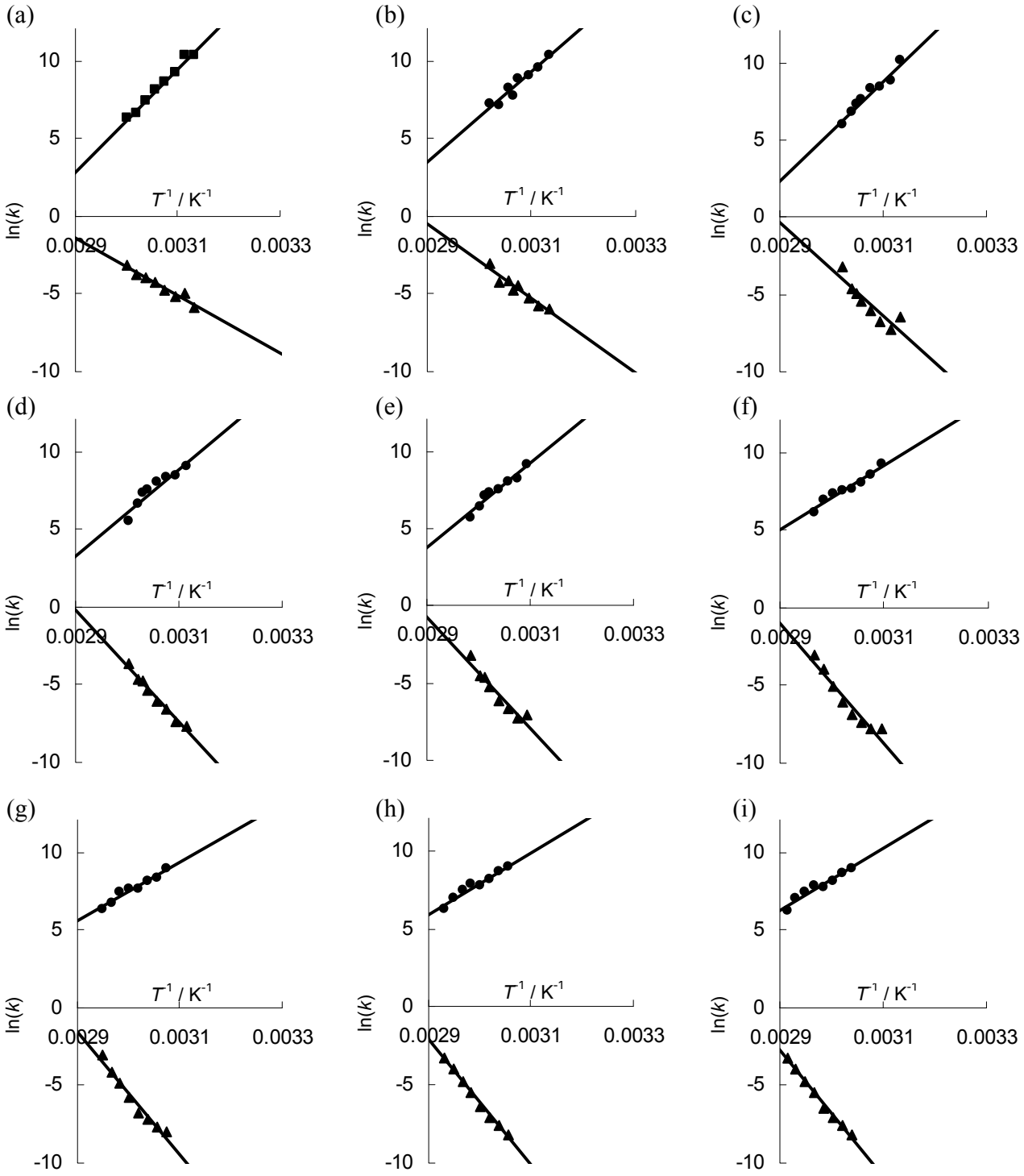

Figure S2-5. Arrhenius plots of S9-S10 of (●) association and (▲) dissociation for (a) batchwise or microchannel flow state at (b) 0.7 cm s^{-1}, (c) 1.7 cm s^{-1}, (d) 2.3 cm s^{-1}, (e) 3.3 cm s^{-1}, (f) 4.2 cm s^{-1}, (g) 5.0 cm s^{-1}, (h) 5.8 cm s^{-1}, and (i) 6.7 cm s^{-1}. The lines are least-squares fits of the data.

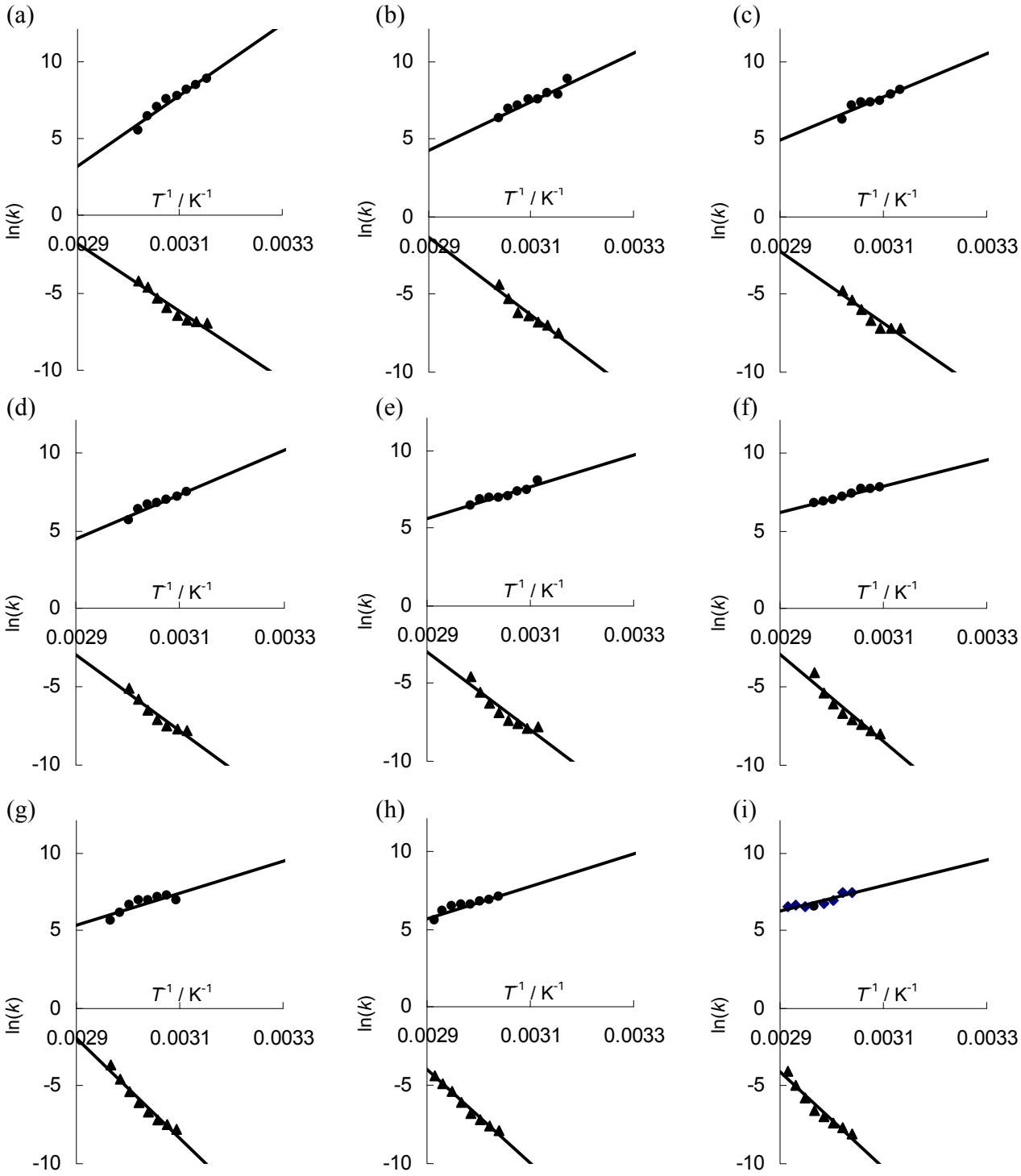

Figure S2-6. Arrhenius plots of S11-S12 of (●) association and (▲) dissociation for (a) batchwise or microchannel flow state at (b) 0.7 cm s^{-1}, (c) 1.7 cm s^{-1}, (d) 2.3 cm s^{-1}, (e) 3.3 cm s^{-1}, (f) 4.2 cm s^{-1}, (g) 5.0 cm s^{-1}, (h) 5.8 cm s^{-1}, and (i) 6.7 cm s^{-1}. The lines are least-squares fits of the data.

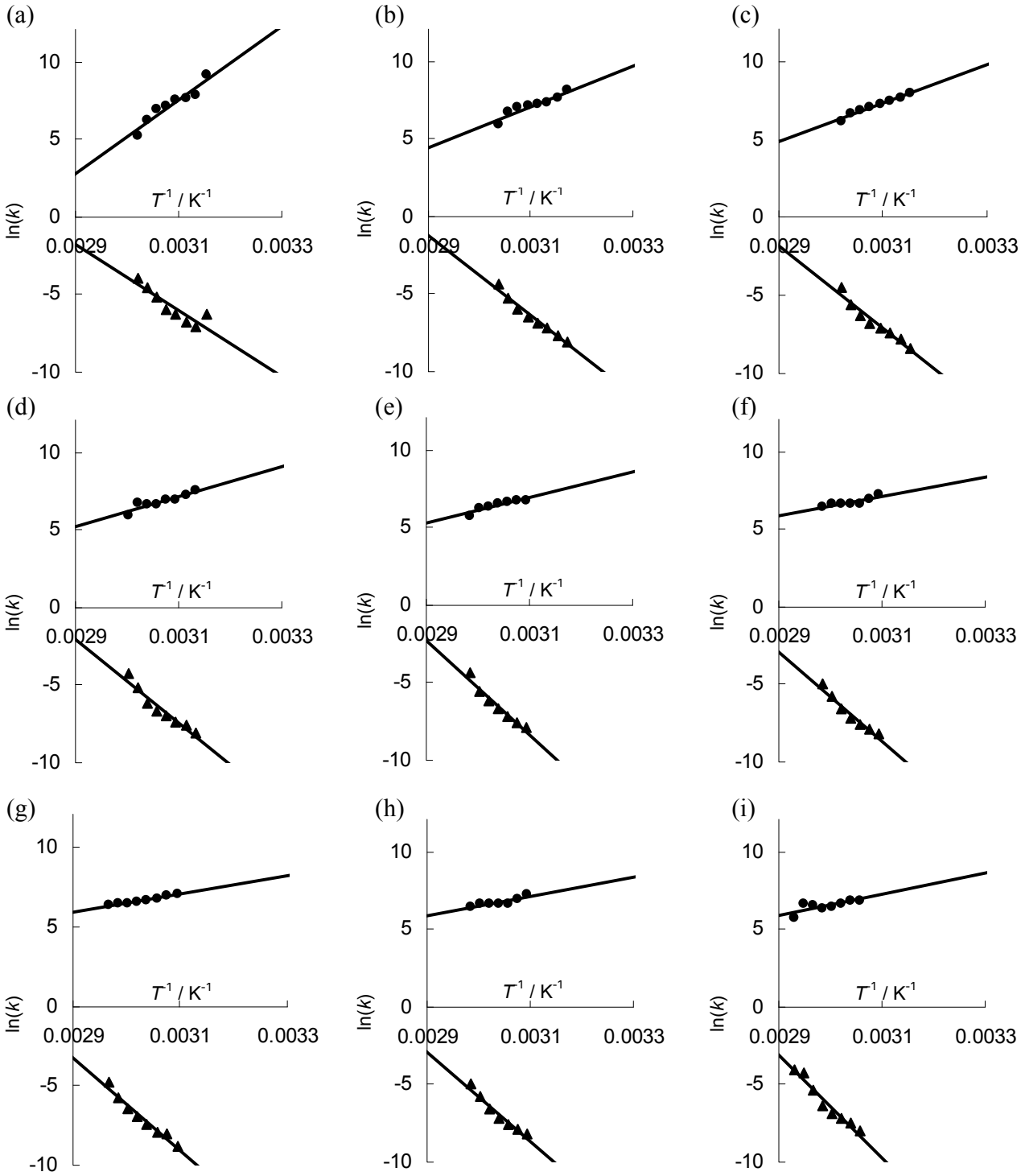

Figure S2-7. Arrhenius plots of S13-S14 of (●) association and (▲) dissociation for (a) batchwise or microchannel flow state at (b) 0.7 cm s^{-1}, (c) 1.7 cm s^{-1}, (d) 2.3 cm s^{-1}, (e) 3.3 cm s^{-1}, (f) 4.2 cm s^{-1}, (g) 5.0 cm s^{-1}, (h) 5.8 cm s^{-1}, and (i) 6.7 cm s^{-1}. The lines are least-squares fits of the data.

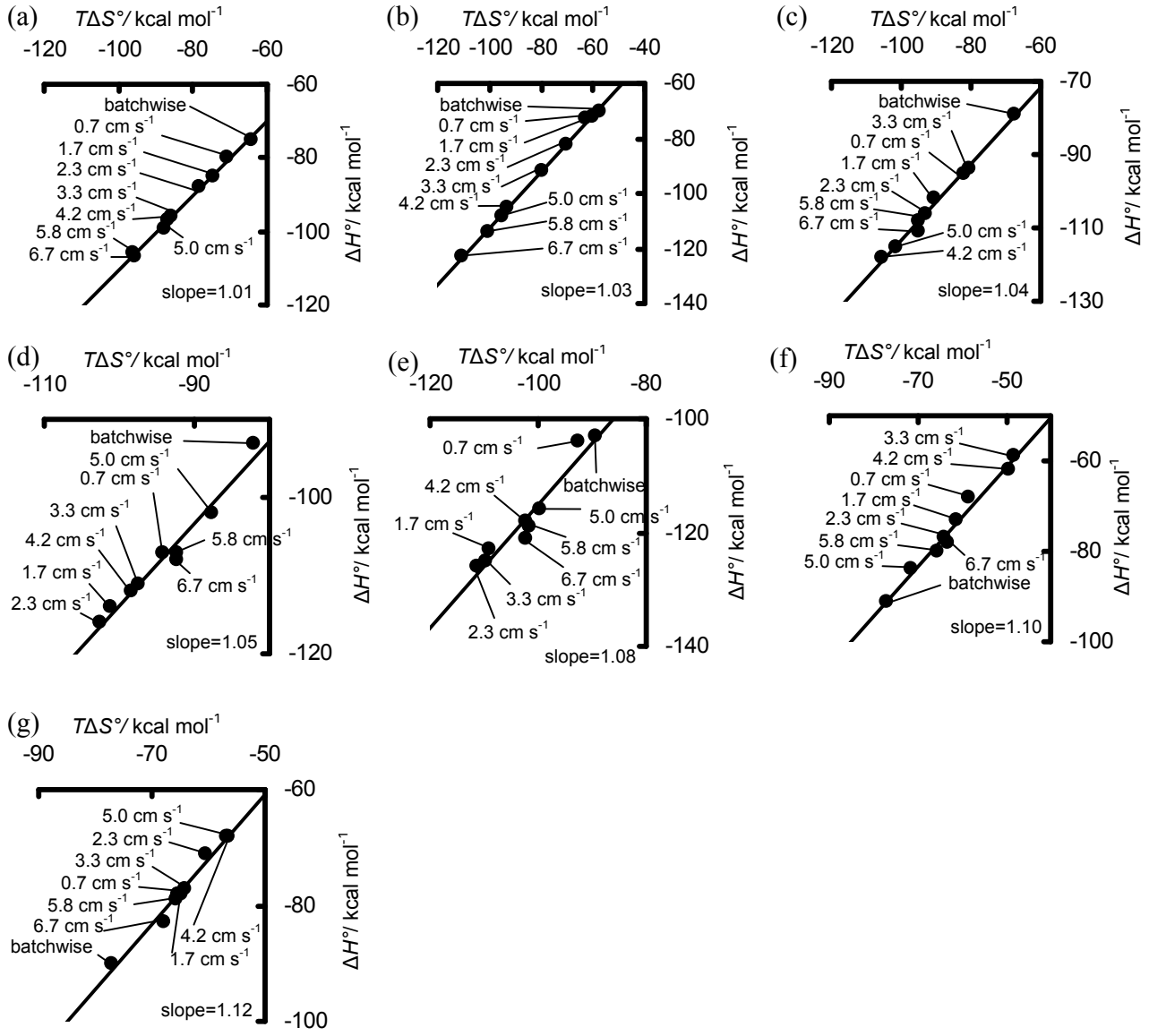

Figure S3. Enthalpy-entropy compensation plots of DNA oligomers (a) S1-S2, (b) S3-S4, (c) S5-S6, (d) S7-S8, (e) S9-S10, (f) S11-S12, and (g) S13-14 for batchwise (cuvette with stirring) and microchannel flow state at 37°C. The lines show least-squares fits of the data.